COBEM 2023 27TH INTERNATIONAL CONGRESS OF MECHANICAL ENGINEERING

ABCM Brazilian Society of Mechanical Sciences and Engineering
27th ABCM International Congress of Mechanical Engineering
December 04-08, 2023, Florianópolis-SC, Brazil

COB-2023-0641
STUDY OF THE IMPACT OF HARMONIC ATUATION ON LAMINAR SEPARATION BUBBLES ON AN AIRFOIL

Marcos Paulo Ziola de Nardo
Leandra Abreu
Daniel Sampaio Souza
Elmer Mateus Gennaro
São Paulo State University (UNESP), Campus of São João da Boa Vista, São João da Boa Vista, SP, Brazil
marcos.nardo@unesp.br
leandra.abreu@unesp.br
daniel.s.souza@unesp.br
elmer.gennaro@unesp.br

Abstract. *Flow separation is a critical issue in aerodynamic applications, causing various harmful effects like increased pressure fluctuations, stall, and loss of lift, ultimately leading to increased fuel consumption. To mitigate this problem, periodic excitations have been studied for separation control, which has shown promising results for flow reattachment, performance, and optimization. Exciting Kelvin-Helmholtz instabilities in the shear layer formed from the point of separation is considered the fundamental mechanism for suppressing flow separation. In this study, we investigate the impact of external disturbances on laminar separation bubbles and their potential to amplify nonlinear phenomena and promote transition to turbulence. We conducted simulations using computational fluid dynamics on NACA0012 at varying angles of attack, and we identified the presence of separation bubbles by analyzing the wall shear stress. We performed RANS simulations using the kω-SST turbulence model and analyzed the velocity and pressure fields around the airfoil, as well as the aerodynamic forces and surface pressure from steady-state simulations. Our results indicate that the introduction of disturbance waves affected the aerodynamic coefficients of the airfoil.*

Keywords: *Aerodynamics, CFD, RANS, Laminar Separation Bubble*

1. INTRODUCTION

The aerodynamics of airfoils are relevant in many applications, such as different kinds of vehicles and energy systems. With the advancement of computers, the computational part of aerodynamics, named CFD (Computational Fluid Dynamics), also advanced. However, as aviation problems generally require a high computational cost (Ferziger and Peric, 2012), even according to the current technological development, alternatives for cheaper and simplified simulations were studied. There are three different types of simulations in CFD, each with its computational cost and respective degree of fidelity: the DNS simulation (Direct Numerical Simulation) is the one that presents the closest results to reality. However, the aggregate computational cost is extremely high, which ends up being restricted to a few studies; intermediately, the LES simulation (Large-eddy Simulation) focuses on solving and calculating large-scale eddies, which ends up simplifying the solution and making the computational cost significantly lighter; Finally, the simulation that has the lowest computational cost is RANS (Reynolds-average Navier Stokes), which calculates the average properties of the set of Navier-Stokes equations with the help of turbulence models, and is widely used academically and industrially.

In aerodynamic applications, flow separation can cause structural fatigue due to increased pressure fluctuations and stall (Yeh and Taira, 2019). As a result of the latter, several other events occur, such as loss of lift and an increase in drag and noise, which in turn cause an increase in fuel consumption and discomfort on the part of passengers.

With this in mind, forms of flow control have been studied over the years, starting with the passive form from geometric changes in the object of study and then the active form, using periodic perturbations with defined frequency through jets of water—air, sound waves, thermal, or others. For separation control, periodic excitations have shown a better capacity for flow reattachment and optimization of aerodynamic performance (Zaman *et al.*, 1989). In turn, Greenblatt and Wygnanski (2000) provided an overview of the use of periodic excitation to control flow separation by suggesting that the fundamental mechanism for the suppression of separation lies in the excitation of Kelvin-Helmholtz instabilities in the shear layer formed from the point of separation.

In line with the rapid advancements in the aeronautical sector, the pursuit of increased speed in aircraft led to the adoption of sleeker aerodynamic profiles and reduced wing areas. However, these changes had a direct impact on the critical aspect of stall conditions – the loss of lift due to the separation of airflow from the wing. This was a subject that, at

the time, lacked an in-depth understanding. Between 1940 and 1950, the National Advisory Committee for Aeronautics (NACA) dedicated substantial efforts to research the phenomena associated with stalls. These stalls were traditionally attributed to the separation of airflow near the wing's leading edge. '

Flow separation in low Reynolds number regimes, as mentioned earlier, plays a crucial role in the dynamics of lifting surfaces. One specific separation phenomenon of notable interest is the formation of the laminar separation bubble (LSB), which occurs near the leading edge of thin airfoils as the angle of attack increases. This separation of the laminar boundary layer takes place just upstream of the point of maximum suction on the airfoil's upper surface due to an adverse pressure gradient.

The resulting separated flow layer encompasses a region with slow-moving recirculating flow, often referred to as the "dead air" region. In this environment, hydrodynamic instability takes control of the separated layer's dynamics, significantly amplifying external disturbances. This, in turn, leads to the transition of the flow layer from a laminar state to a turbulent state, even under conditions of low free-stream turbulence.

Low Reynolds number laminar separation bubbles are a common occurrence in various flow situations, making this research highly relevant both in practical applications and for addressing fundamental theoretical questions related to the primary and secondary mechanisms of self-excited instability in such flows. A substantial portion of the literature on this topic, especially experimental and purely numerically simulated studies, has traditionally operated under the assumption that the instability processes and the transition to turbulence within separation bubbles are predominantly driven by the amplification of perturbations from the external fluid field surrounding the bubble itself. However, the findings presented in this study establish the presence of a sequence of flow instabilities and bifurcations that are entirely self-excited by the flow itself Rodríguez *et al.* (2013); Rodríguez and Gennaro (2014); Gennaro *et al.* (2015); Rodríguez *et al.* (2021).

The aim of the work described here is to investigate, through Reynolds-averaged Navier-Stokes (RANS) simulations and unsteady RANS (URANS), the impact periodic of a separation bubble and its control on the aerodynamic of an airfoil and the effect of the periodic excitations on the dynamics of the bubble.

2. METHODOLOGY

2.1 Computational model

This study focuses on an airfoil that has broad applications in research, making it easier to compare and verify the results. The 4-digit NACA profiles are commonly used as they provide a substantial amount of aerodynamic data in the literature. Therefore, the NACA 0012 airfoil was chosen to simplify calculations and simulations.

In order to create the computational model, a computational domain surrounding the object of study is required. This domain will serve as the space in which the flow, such as air, will be simulated to flow over the airfoil. In this case, we have chosen the "O" mesh geometry for the model/domain due to its ease of implementation in the software. The final geometry of the model with the proposed dimensions is depicted in Fig. 1.

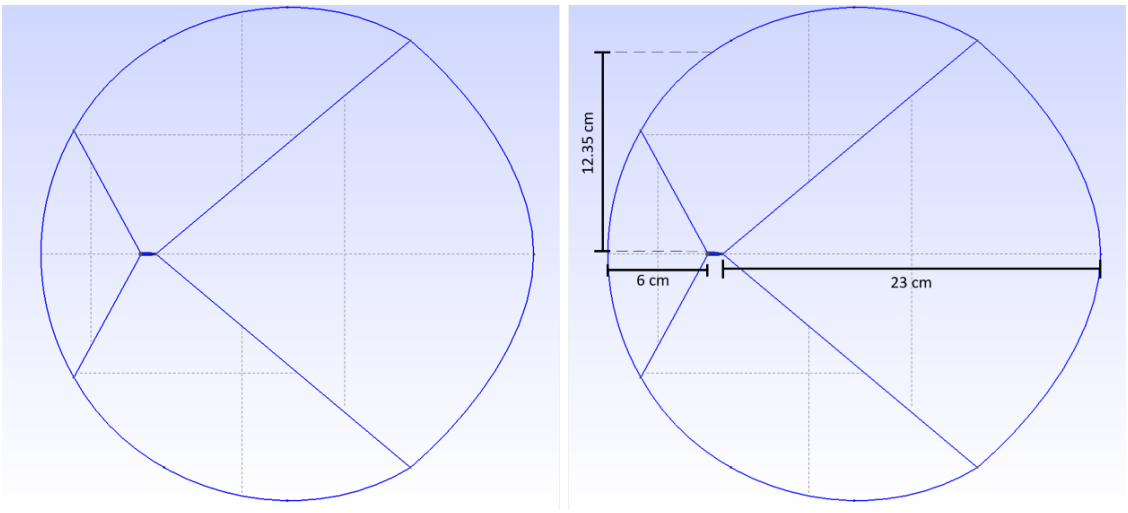

Figure 1. Model Geometry

The geometry of the object of study was elaborated and a structured mesh was built using the stretching method, namely, the mesh has a greater length in the region most external to the object and compresses as it approaches the airfoil. This optimized the simulation by discretizing and concentrating the heavy regions in the most significant area of interest. The final shape of the mesh can be viewed in Fig. 2.

To validate the mesh, a mesh convergence study was carried out with three meshes of different discretizations and the

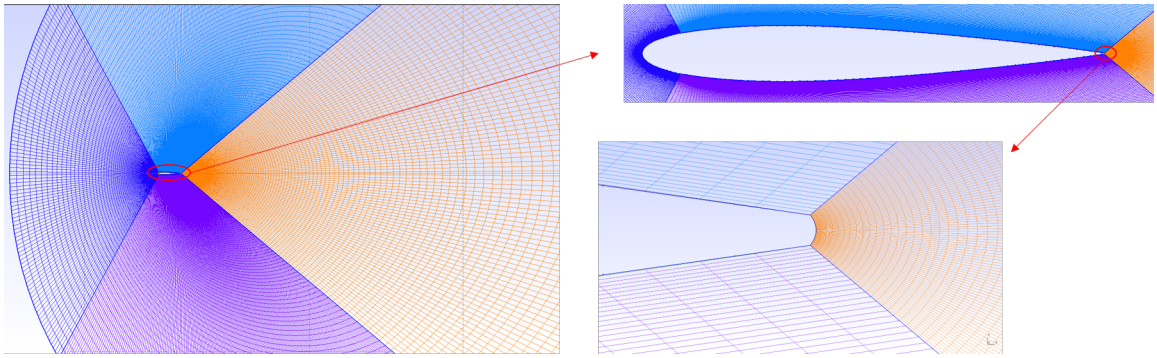

Figure 2. Final Model View

same type of mesh (O) with the same stretching methodology. Tab. 1 shows the values of the numbers of nodes and cells for each mesh and the lift coefficient results obtained.

Table 1. Mesh convergence study.

Mesh name	Number of nodes	Number of cells	Lift Coefficient(1)
Mesh 1	80k	40k	0,0169
Mesh 2	170k	85k	0,0013
Mesh 3	250k	125k	0,0007

(1) Angle of Attack = 0°

The problem-solving methodology was based on a feedback system of initial simulation results. Initially, potential flow was simulated on the object of study, and the resulting permanent simulation was fed by inputs to optimize the simulation time. The results from the permanent simulation were used to obtain the flow separation point and provide the pressure and velocity fields as input parameters for the transient simulation.

For the transiten simulation, two time-varying simulations are performed. The first one does not have any type of disturbance and aims to serve as a reference for comparison of the results obtained later. For the perturbed simulation, which has a perturbation inserted from a variable boundary condition, it was necessary to build a new mesh. In this mesh, a section of the airfoil, before the flow separation point, would be the place of insertion of the perturbation. This was done to carry out an active control of the flow in question. The flow of the processing methodology is visually illustrated in Fig. 3.

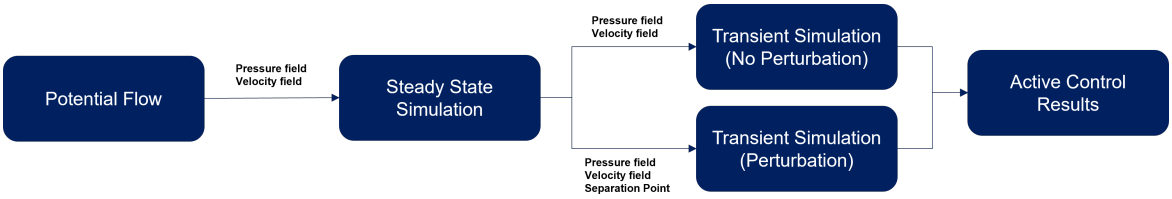

Figure 3. Processing Methodology.

The OpenFoam software was used for all simulation steps shown in Fig. 3, which has various solvers from CFD to thermal, mechanical, and chemical simulation, as well as numerical and algorithm control schemes.

2.2 Flow conditions

The main characteristics adopted for the simulation started from the choice of the Reynolds number equal to 10^5. Concerning the parameters used in the simulations, the variation of the angle of attack used for this work stands out. Since the mesh modification is very laborious and would need to be changed in every simulation that was to be carried out, it was decided to use a single mesh and modify the angle of attack from the decomposition of the velocity inserted in the domain. Since the magnitude of the velocity adopted would always be unitary and the model studied is two-dimensional, the horizontal component of velocity (U_x) is calculated by the cosine of the angle. In contrast, the sine calculates the vertical velocity component (U_y). Therefore, an automated spreadsheet was built to calculate the velocity components representing the desired angle, whose values are represented in the Tab. 2.

Regarding the parameters used in the simulations, the Reynolds number chosen was 10^5. The angle of attack was varied using a single mesh, and the components of velocity that represent the desired angle were calculated by the automated

spreadsheet built for this purpose. The values of the velocity components are shown in Tab. 2.

Table 2. Calculation of velocity components from the desired angle of attack.

Angle of Attack$^{(1)}$	U_x	U_y
0°	1.000000	0.000000
5°	0.996195	0.087156
10°	0.984808	0.173648
15°	0.965926	0.258819
20°	0.939693	0.34202

The simulation results provide force coefficients based on surface normal vectors, while lift and drag coefficients are calculated using flow normal vectors. To obtain accurate values of the coefficients, it's necessary to convert them using Equations (1) and (2).

$$Cd = C_{fx}cos(\alpha) + C_{fy}sin(\alpha) \tag{1}$$

$$Cl = C_{fy}cos(\alpha) - C_{fx}sin(\alpha) \tag{2}$$

2.3 Turbulence Models

This study explores the Spalart-Almaras and K-ω SST models, which are well-known for their simplicity and ability to capture physical phenomena near the boundary layer. By providing more information on the models' strengths and limitations, readers gain a better understanding of their relevance to the research (Wauters and Degroote, 2018; Allmaras and Johnson, 2012; Spalart and Allmaras, 1992; Menter *et al.*, 2003).

To compare the performance of these models, an analysis was conducted with three different angles of attack: $0°$, $4°$, and $15°$. The results were compared to experimental values from NASA (2021) and plotted in Fig. 4. It was observed that the K-ω SST model had values closer to the experimental ones, making it the preferred turbulence model for both steady state and transient simulations.

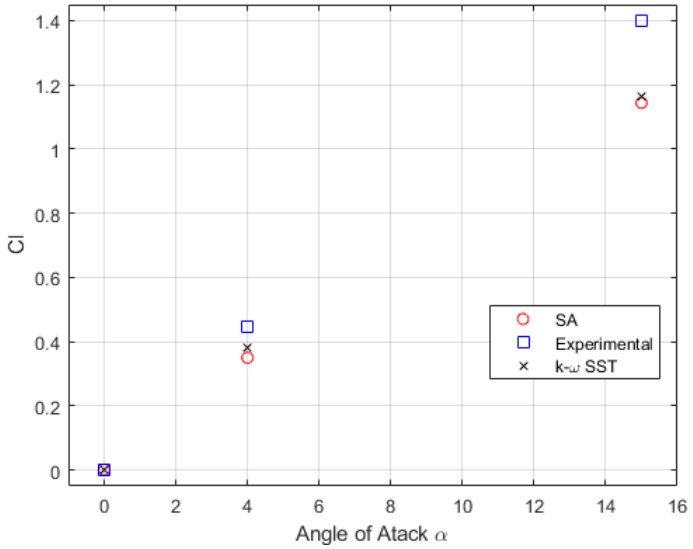

Figure 4. Comparison of Spalart-Allmaras and K-ω SST models.

Paraview is a powerful software that allows for visual analysis of simulation results obtained from OpenFoam. With its ability to insert calculations based on the physical properties of the flow, such as velocity, pressure, and viscous tension, Paraview makes it possible to calculate various aerodynamic characteristics. For instance, one can easily calculate the coefficient of friction and pressure on the airfoil since they depend on the software's internal fields like pressure field and viscous tension, respectively. Overall, Paraview provides an efficient way to analyze and understand the results of complex simulations.

2.4 Separation Point Identification

The simulations carried out and processed by Paraview, a post-processing software, provide valuable data that can be used to calculate the coefficients of force, pressure, and friction on the airfoil surface. The authors have developed an algorithm in Python language that facilitates this process.

According to Cebeci *et al.* (1972), the point at which the coefficient of friction on the contact surface is zero represents the separation point of a flow. Moreover, the region where the coefficient is positive indicates the separation of the flow over the surface. Additionally, Mitra and Ramesh (2019) highlights the correlation between the formation of a separation bubble and the presence of a plateau in the airfoil pressure coefficient curve.

3. RESULTS

3.1 Steady State Solution

The study conducted involved steady-state simulations which helped obtain the coefficients of forces, pressure, and viscous tension. The velocity and pressure fields of the airfoil were also observed during the simulations. These values were then used as input for the forced simulations to facilitate the convergence process and compare the coefficient outputs.

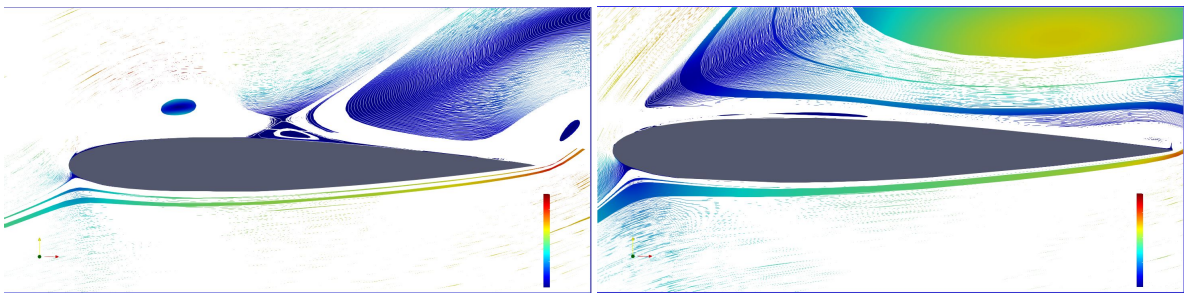

Figure 5. Streamlines at Angle of Attack = 15° and 20°.

The force coefficients of the airfoil were obtained through a simulation performed in OpenFOAM software and post-processing using a code developed in Python language. The text files generated by the simulation were imported, and the final values were calculated using equations (1) and (2).

Table 3. Force coefficients results.

Angle of Attack	Lift coefficient	Drag coefficient
0^o	-0.000559	0.0159
5^o	0.473	0.0206
10^o	0.855	0.0387
15^o	0.635	0.217
20^o	0.718378	0.332

Comparing the values obtained from the simulation, Tab. 3, with the experimental data obtained by Zafi *et al.* (2020) and the simulation performed in XFLR5 software, it was observed that the values from the simulation were very close to the experimental values for angle of attack values smaller than 15°. This indicates that the flow was mostly attached to the airfoil surface. However, for the coefficient values for AoA = 15° and AoA = 20°, where recirculation zones were observed, Fig. (5a) and Fig. 5(b), the values from the simulation were intermediate between the experimental and XFLR5 values.

As for the pressure and friction coefficient curves along the airfoil's upper surface, they were plotted to verify whether there is separation and, once identified, whether or not there is reattachment and at which point this phenomenon occurs. Figures (7) and (8) are a representation of the mentioned curves for the angle of attack 10°.

To check for separation and reattachment, the pressure and friction coefficient curves along the airfoil's upper surface were plotted. The point of separation of the flow over an object can be identified from a plateau on the airfoil pressure curve or in the region where the coefficient of friction is zero. In the case of the study, the separation of the flow occurred in the region close to the leading edge, approximately between 1% and 5% of the chord. A laminar separation bubble was formed between 17% and 41% of the chord when AoA = 15°. Similarly, when AoA = 20°, the region from approximately 59% of the chord was highlighted, where the friction coefficient values were negative.

3.2 Transient Solution

After conducting numerical simulations where we varied the frequency and amplitude, as shown in Tab. 4, we observed an invariance between the imposed parameters of simulations 2 to 5. Therefore, we chose to compare the results for undisturbed simulations with disturbance simulation 4, based on the outcomes obtained.

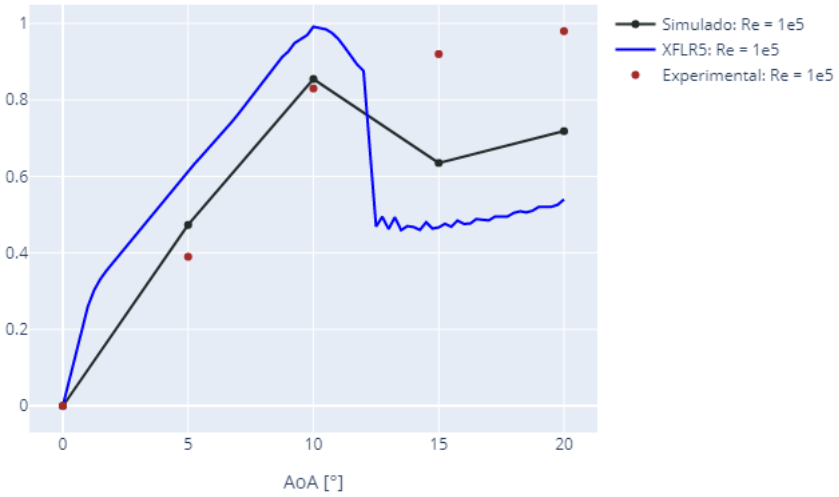

Figure 6. Lift coefficient according to angle of attack.

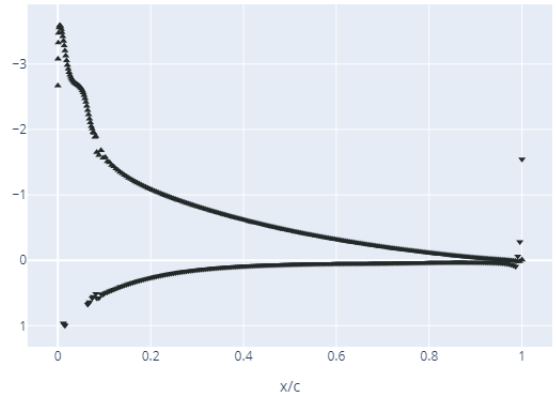

Figure 7. Pressure coefficient at Angle of Attack = 10°.

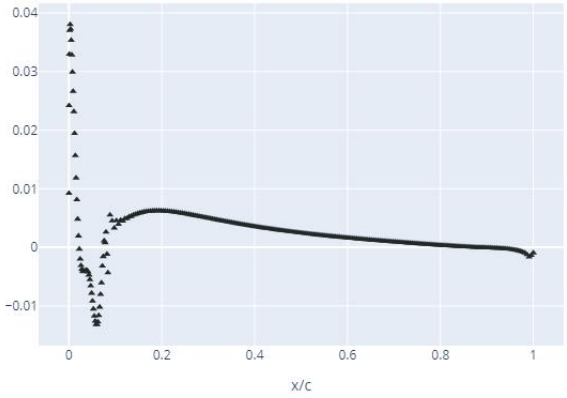

Figure 8. Friction coefficient at Angle of Attack = 10°.

Since the values for AoA = 0° is very close to 0, the division between the comparative terms generates very high percentages. Therefore, the calculation for such an angle is disregarded. Thus, it appears that the comparative values of the disturbed simulations are only effective when there are laminar separation bubbles or even separation of the flow over the airfoil, which occurs for angles of attack AoA = 15° and AoA = 20°. As observed in Tab. 5, for these two angles, there is an increase in the value of the lift coefficient and a decrease in the value of the drag coefficient, both positive phenomena.

Table 4. Sensitivity of the perturbation parameters on the simulation performed for AoA = 10°.

Name	Frequency	Amplitude
Disturbed Simulation 1	0.005	0.016
Disturbed Simulation 2	0.005	0.0001
Disturbed Simulation 3	0.005	0.00001
Disturbed Simulation 4	0.0005	0.00001
Disturbed Simulation 5	0.05	0.00001

Table 5. Comparison between permanent and disturbed simulation.

Angle of Attack	Lift Coefficient	Drag Coefficient	Aerodynamic efficiency (C_l/C_d)
0^o	+ 102%	+ 155%	-21%
5^o	- 65%	+ 137%	-85%
10^o	- 52%	+ 118%	-78%
15^o	+ 15%	- 23%	+49%
20^o	+ 55%	- 4%	+62%

4. FINAL REMARKS

In this study, the amplification of perturbations in separation bubbles was examined, specifically, the active control of the flow through the insertion of perturbations in the model. The research was conducted using OpenFOAM, an open-source software, with the solvers of steady-state (*simpleFoam*) and transient regime (*pisoFoam*), as well as other software like XFLR5, which was used to calculate two-dimensional inviscid simulations, and *Paraview*, responsible for the post-processing of the simulations.

The results obtained from the permanent simulations showed the formation of separation bubbles and the location of the separation and reattachment points. Although the simulated values are very close to lower angles of attack when compared with experimental data, it is important to note that the presence of non-linear phenomena, such as the separation bubble, allows more significant divergences concerning the experimental values due to the models of the computational solution adopted. Moreover, the velocity and pressure fields visualization on the airfoil helped identify recirculation zones and flow separation bubbles, which, together with the numerical results, confirmed the studied phenomena.

The application of a disturbance on the flow caused a worsening in the results for low angles of attack since the disturbance ends up causing instabilities in the boundary layer region. However, the disturbance can help in the fluid flow reattachment when there are stronger pressure peaks near the leading edge, which causes an increase in the lift coefficient and a decrease in the drag coefficient since separation tends to occur closer to the trailing edge of the airfoil.

Since the simulations calculated from simplified software such as XFLR5 are insufficient and distant from the real values, and the realization of an experiment that faithfully represents the physics of the problem is expensive and extremely difficult, the use of CFD simulations is plausible and necessary for the general industry. Even with numerical errors, the models produced and calculated through computational fluid aerodynamics are satisfactorily close to the real results, as seen in this study.

5. ACKNOWLEDGEMENTS

This work is supported by São Paulo Research Foundation (FAPESP) grants 2023/14104-4, 2014/24782-0 and 2017/01586-0.

6. REFERENCES

Allmaras, S.R. and Johnson, F.T., 2012. "Modifications and clarifications for the implementation of the spalart-allmaras turbulence model". In *Seventh international conference on computational fluid dynamics (ICCFD7)*. pp. 1–11.

Cebeci, T., Mosinskis, G.J. and Smith, A.M.O., 1972. "Calculation of separation points in incompressible turbulent flows". *Journal of Aircraft*, Vol. 9, No. 9, pp. 618–624.

Ferziger, J.H. and Peric, M., 2012. *Computational methods for fluid dynamics*. Springer Science & Business Media.

Gennaro, E.M., Rodríguez, D. and Souza, L.F., 2015. "Secondary instability analysis of 3d laminar separation bubbles based on cross-plane wkb approximation". In *Proceedings of 23rd ABCM International Congress of Mechanical Engineering*.

Greenblatt, D. and Wygnanski, I.J., 2000. "The control of flow separation by periodic excitation". *Progress in aerospace Sciences*, Vol. 36, No. 7, pp. 487–545.

Menter, F.R., Kuntz, M. and Langtry, R., 2003. "Ten years of industrial experience with the sst turbulence model". *Turbulence, heat and mass transfer*, Vol. 4, No. 1, pp. 625–632.

Mitra, A. and Ramesh, O., 2019. "New correlation for the prediction of bursting of a laminar separation bubble". *AIAA Journal*, Vol. 57, No. 4, pp. 1400–1408.

NASA, 2021. "Turbulence modeling resource". URL `https://turbmodels.larc.nasa.gov/naca0012_val_sst.html`.

Rodríguez, D., Gennaro, E.M. and Souza, L.F., 2021. "Self-excited primary and secondary instability of laminar separation bubbles". *Journal of Fluid Mechanics*, Vol. 906, p. A13. doi:10.1017/jfm.2020.767.

Rodríguez, D. and Gennaro, E.M., 2014. "On the secondary instability of forced and unforced laminar separation bubbles". *Procedia IUTAM*, Vol. 14, pp. 78 –87. Presented at IUTAM-ABCM 8th Symposium on Laminar Turbulent Transition.

Rodríguez, D., Gennaro, E.M. and Juniper, M.P., 2013. "On the two classes of global primary modal instability in laminar separation bubbles". *AIAA-paper*, , No. 2013-. Presented at AIAA Fluid Dynamics Conference and Exhibit, 43rd.

Spalart, P. and Allmaras, S., 1992. "A one-equation turbulence model for aerodynamic flows". In *30th aerospace sciences meeting and exhibit*. p. 439.

Wauters, J. and Degroote, J., 2018. "On the study of transitional low-reynolds number flows over airfoils operating at high angles of attack and their prediction using transitional turbulence models". *Progress in Aerospace Sciences*.

Yeh, C.A. and Taira, K., 2019. "Resolvent-analysis-based design of airfoil separation control". *Journal of Fluid Mechanics*, Vol. 867, pp. 572–610.

Zafi, N.A., Hossain, M.A. and Mim, M.T.I., 2020. "Experimental study of naca 0012 airfoil with slanted drills through the body".

Zaman, K., McKinzie, D. and Rumsey, C., 1989. "A natural low-frequency oscillation of the flow over an airfoil near stalling conditions". *Journal of Fluid Mechanics*, Vol. 202, pp. 403–442.

7. RESPONSIBILITY NOTICE

The authors are solely responsible for the printed material included in this paper.